主論文

$^{87}Sr/^{86}Sr$ variation in north Pacific sediments: A record of the Milankovitch Cycle in the past 3 million years

（北太平洋堆積物の $^{87}Sr/^{86}Sr$ 比の変動：過去 300 万年間のミランコビッチサイクルの記録）

浅 原 良 浩

Earth and Planetary Science Letters

(1999, in press)

Accepted for publication in the Earth and Planetary Science Letters

14 June 1999

$^{87}Sr/^{86}Sr$ variation in north Pacific sediments: A record of the Milankovitch Cycle in the past 3 million years

Yoshihiro Asahara

Department of Earth and Planetary Sciences, Graduate School of Science, Nagoya University, Chikusa, Nagoya 464-8602, Japan

Tel: +81-52-789-2530

FAX: +81-52-789-3033

E-mail: asahara@eps.nagoya-u.ac.jp

Abstract

Temporal variations of Sr isotopic compositions in the detrital component of north Pacific sediments have been precisely examined. The Sr isotopic composition is controlled by the flux of eolian material from the Asian continent with a high $^{87}Sr/^{86}Sr$ ratio (0.724 - 0.726) relative to volcanic material with a low ratio (0.703 - 0.705) from the Izu-Ogasawara-Mariana arc and oceanic islands such as Hawaiian Islands. Assuming that the volcanic flux is constant, the temporal variation in Sr isotopic ratio reflects the amount of eolian input from the continent. The major characteristics of the temporal variations and the interpretation of them are summarized as follows: (1) The $^{87}Sr/^{86}Sr$ records show cyclic fluctuations of 400 ky and 100 ky periodicities which are associated with the eccentricity of the earth's orbit (Milankovitch Cycle). (2) Between 3 and 0.8 Ma, the $^{87}Sr/^{86}Sr$ ratio in the north central Pacific sediment increases gradually. This reflects an increased eolian input from the arid region in east Asia. The increase must be related to aridification of the Asian continent. (3) The decreased $^{87}Sr/^{86}Sr$ ratio during the past 0.8 my implies a decreased eolian input. The age of 0.8 Ma may relate to the climatic event known as the middle Pleistocene shift. All of these phenomena reflect a fluctuation of the eolian flux corresponding to the paleoclimatic cycle of aridity in the Asian continent. The Sr isotopic composition of pelagic sediment in the north Pacific is sensitive to changes in the eolian input reflecting to the aridity of the Asian continent.

keywords: $^{87}Sr/^{86}Sr$; Pacific sediment; Milankovitch Cycle; Asian loess; paleoclimate

1. Introduction

Most studies of Quaternary climates have focused on changes in $\delta^{18}O$ and $\delta^{13}C$ in the $CaCO_3$ of foraminiferal shells (e.g., [1]), carbonate content in sediments (e.g., [2]) and the magnetic susceptibility of sediments (e.g., [3-5]). Recently, paleo-environmental analysis using radiogenic isotopes in the detrital fraction of marine sediment has been carried out. For example, Sr-Nd isotopes are used as tracers of deep water and surface water currents in South-Barbados [6] and in the North Atlantic [7, 8]. The Sr and Nd isotopic compositions of the detrital fraction are valuable indicators of source-region material (e.g., [9-11]). Temporal variation of the radiogenic isotopes will provide information on both paleoclimatic variations in the source region and geologic events.

We recently found that the areal distribution of $^{87}Sr/^{86}Sr$ ratios in north Pacific surface sediments is controlled by the mixing of two major components, i.e., a continental component with a high $^{87}Sr/^{86}Sr$ ratio and a volcanic component with a low ratio (Fig. 1; [12]). In particular, the $^{87}Sr/^{86}Sr$ ratio is high in north central Pacific sediments, which have deposited away from areas of river input and ice rafting. The high ratio indicates the signature of the Asian continental material, loess [12, 13]. The Asian loess is carried into the north Pacific by middle-latitude westerlies and beyond, as far as Greenland [14]. The vertical variation in Sr isotopic composition of core samples is then expected to reveal paleoclimates in the Asian continent such as aridity, glaciation and atmospheric circulation of the Northern Hemisphere. In this study, temporal variations of Sr isotopic compositions in detrital component of north Pacific sediments have been precisely examined. The most striking observation from the records is the existence of a cyclic fluctuation with the periodicities associated with the Milankovitch Cycle during the Quaternary. The eolian flux from the Asian continent into the

north Pacific is related to the aridity of the Asian source region and is sensitively reflected by the $^{87}Sr/^{86}Sr$ ratios of pelagic sediments.

2. Samples

Vertical variations of Sr isotopic composition were examined at three locations in the north Pacific (Fig. 1). Three cores were obtained during the NH91-1 and the NH93-1 cruises of the R/V *Hakurei-maru*. Two locations, NGC55 and NP18, are in the north central Pacific and the other, NP29, is in the western north Pacific close to the Mariana arc. NP18 and NP29 are piston cores and NGC55 is gravity core. The water depths of the coring sites are deeper than 5000 m, which is below the CCD. Then, these sediments do not contain any carbonate. The three cores were not included in the previous study of strontium isotope distribution of surface sediments [12]. Details of mineralogical and morphological descriptions on the three sites were published elsewhere [5, 15, 16] and are summarized in Table 1.

NGC55 is a core sample taken in close vicinity of NB69 of Asahara et al. [12]. The core consists of dark brown to dark reddish brown clay, and 196 samples were examined there. The samples cover the age of 0 to 3.1 Ma. NP18 is taken in proximity to NB37 [12]. The core is composed of brown to dark brown clay, and 114 samples were examined. The samples cover the age of 0 to 3.6 Ma. NP29 is taken from the location close to NB50 [12]. The core contains brown to dark brown clay and 205 samples were examined. The samples cover the age of 0 to 6.3 Ma. NB69, NB37 and NB50 are surface sediments and their $^{87}Sr/^{86}Sr$ ratios are 0.7191, 0.7188 and 0.7129, respectively. The high Sr isotopic ratios of the former two locations clearly reflect the strong supply of the Asian loess to the sediments. The surface sediment of the latter location partially reflects the volcanics supplied from the

Mariana arc and oceanic islands.

The ages of these core samples have been determined by magnetostratigrapy [5, 17]. Ages of geomagnetic polarity reversals follow Berggren [18]. Ages between boundaries of geomagnetic reversals are determined on the assumption that the sedimentation rate of each interval is constant. The age before 3.58 Ma of NP18 core is not known because of unstable remnant magnetization. As shown later, fluctuation patterns of Sr isotopic ratios in the three core samples during the period 0.8 - 0 Ma are quite similar to each other and therefore the shift of age of cores due to missing of core-tops and/or bioturbation is small, if any. Then the core-tops are assumed to be zero age.

The sampling interval of each core is usually 2 cm, but partly 1 or 10 cm, and a sample of 1 cm in thickness is taken at every sampling point. Average linear sedimentation rates for the cores range from 0.5 to 1.2 mm ky^{-1}. Benthic fauna continuously reworks ocean-floor sediments after their deposition and further smear temporally fluctuating sedimentary signals. Each Sr isotopic ratio, then, is an integrated representation of at least 8 ky of deposition processes. The sedimentation rates of 0.5 - 1.2 mm ky^{-1} and a sampling interval of 2 cm provide a temporal resolution of 17 - 40 ky.

The velocity of the Pacific plate motion is about 10 cm y^{-1} and, therefore, sample locations move at about 100 km my^{-1}. Change in the distance between the sampling localities and the Asian source region can be disregarded in the following discussion.

3. Analytical procedures

Most of the samples weighed approximately 100 mg. The silicate detritus of each sample was refined by a chemical extraction of authigenic material using 0.25N-hydrochloric

acid for 1 hour. The detrital residue was washed several times with ultrapure distilled and deionized water. This leaching procedure does not affect the isotopic ratio of the detrital fraction [12]. HCl-treated residue, defined as the detrital component, was decomposed by hydrofluoric acid and perchloric acid. Strontium was separated from the major elements using a AG50W-X8 cation exchange resin.

Sr isotopic compositions were measured with a VG Sector thermal ionization mass spectrometer using dynamic triple collector analyses at the Geological Survey of Japan for NP18 and with a VG Sector 54-30 at Nagoya University for NGC55 and NP29. During the collection of 200 dynamic cycles, the ^{88}Sr ion beam was maintained at 2.0 V (0.020 nA) for VG Sector and at 1.0 V (0.010 nA) for VG Sector 54-30. The average $^{87}Sr/^{86}Sr$ ratios of the NIST-SRM 987 during the course of this study were 0.710244 ± 0.000023 (2σ, n=11) for NP18 and 0.710252 ± 0.000027 (2σ, n=152) for NGC55 and NP29. The ratios of NP18 presented in Table 2 were normalized to the value of the NIST-SRM 987 for NGC55 and NP29.

4. Results

Sr isotopic composition, depth and age are presented in Table 2. The temporal variations in $^{87}Sr/^{86}Sr$ ratio are shown in Figs. 2-a, b and c.

Sr isotopic compositions in the top of the NGC55 and the NP18 cores are consistent with those of the surface sediments in the vicinity, NB69 and NB37 (Tables 1 and 2). The top of the NP29 core has a slightly higher ratio (0.7142) than the NB50 surface sediment (0.7129). Although the sampling points of NP29 and NB50 cores are close, their sedimentary environments are considered to be slightly different. Manganese nodules occur at the surface

of NB50 [16] and do not occur at the surface of NP29.

$^{87}Sr/^{86}Sr$ ratios and their temporal variation patterns of NGC55 and NP18 are quite similar to each other and tend to increase during the interval from 3 to 0.8 Ma, when the highest isotopic ratios reach about 0.720, and tend to decrease during the past 0.8 my. The isotopic ratio of NP29 is lower than those of NGC55 and NP18, and tends to increase slightly from 6 to 2 Ma, when it reaches approximately 0.717, and tends to decrease during the past 0.8 my.

The temporal variations in Sr isotopic composition of the core sediments are compared with the sedimentation rates in Fig. 3 in which the averages of the Sr isotopic ratios and the accumulation rates in each geomagnetic polarity interval are shown. The sedimentation rate (g cm^{-2} ky^{-1}) is calculated, based on the sediment accumulation rate (mm ky^{-1}) and the dry sediment density deduced from the water content and the specific gravity [19, 20]. Estimated sedimentation rates of short polarity intervals, such as 0.78 - 0.99, 0.99 - 1.07 and 1.77 - 1.95 Ma, may not be accurate. In segments with short polarity intervals (< 0.2 my) and low sedimentation rates (< 1.5 mm ky^{-1}), lags of age between the geomagnetic reversals and the deposition may be caused by a relatively viscous nature of the remnant magnetization. Fluctuation patterns of average Sr isotopic ratios of the three cores during the past 3 my are fairly similar to each other, except for a drop in Sr isotopic ratio of NP29 at 1.9 Ma.

5. Discussion

5.1 Long-term trend of fluctuation in $^{87}Sr/^{86}Sr$ ratio

The temporal variation in Sr isotopic ratio of the core sediment dominantly reflects the relative flux of material with a high $^{87}Sr/^{86}Sr$ ratio to one with a low ratio. The material with a high ratio is the eolian dust from the Asian continent (0.724 - 0.726; [21]) and the material with

a low ratio is the volcanics from the Izu-Ogasawara-Mariana arc and oceanic islands, such as the Hawaiian Islands (0.703 - 0.705; [22-25]). Rb-Sr isochron plot for some of the detrital components in the three core samples is shown in Fig. 4 to demonstrate the mixing of the two components [21]. Approximately 15 samples of each core during the period 0 - 3.0 Ma are plotted. The Rb-Sr isotopic systematics of these Quaternary core sediments show a well-correlated pseudo isochron with an age of 300 Ma. This proves the mixing of the two components.

The temporal variations of continental (eolian) and volcanic fluxes for these core samples are calculated as follows. At first, the relative contributions of the continental component are quantitatively calculated for the samples shown in Fig. 4 from the plausible Sr isotopic compositions and concentrations for the continental and the volcanic components. $^{87}Sr/^{86}Sr$ ratios and Sr concentrations for the continental and the volcanic components are regarded as 0.725, 100 ppm and 0.704, 300 ppm, respectively. Relative amounts of the continental component are calculated using Sr isotopic ratios of the samples. Using the relative amounts of the continental and volcanic components and the quantitative sedimentation rates in Fig. 3, the continental and volcanic fluxes (g cm^{-2} ky^{-1}) are calculated. The results are shown in Fig. 5. Both of the calculated fluxes of NP18 at 0.83 Ma are anomalously low. As described above, the sedimentation rate at 0.83 Ma may not be precise enough for the quantitative calculation because of a low sedimentation rate and a short geomagnetic period (0.2 my).

At NP18 and NGC55 in the north central Pacific, the eolian fluxes increase during the period from 3.0 Ma to 0.8 Ma and decrease slightly since 0.8 Ma. The volcanic fluxes of the two cores are almost constant (0.005 and 0.010 g cm^{-2} ky^{-1}, respectively) during the past 3 my.

Then, the fluctuations of $^{87}Sr/^{86}Sr$ ratio of the two core sediments appear to be controlled by the eolian flux.

Around 2.5 Ma, the Earth's climate changed significantly. Ruddiman and Raymo [27] suggested that accelerated uplift of the Himalayan-Tibetan region at about 2.5 Ma caused the change of atmospheric circulation in the Northern Hemisphere, which triggered the growth of continental ice-sheets [28, 29] and loess formation in the Asian continent [30, 31]. The increase of the eolian flux must be related to increased aridification of the Asian continent.

The NP18 core shows an anomalously low $^{87}Sr/^{86}Sr$ ratio at 2.6 Ma (Fig. 2-b). This is caused by a temporarily reduced input of the eolian material, not an increased input of volcanic material. By smear slide analyses of unleached samples, a larger amount of authigenic phillipsite is found at the depth corresponding to 2.6 Ma. If the formation rate of phillipsite is constant, it is considered that a relatively large amount of authigenic phillipsite at 2.6 Ma is caused by a temporarily decreased supply of the continental material, which is consistent with the anomalously low $^{87}Sr/^{86}Sr$ ratio in the detrital component of the NP18. No clear isotopic anomaly, however, is found in NGC55 and NP29 cores simultaneously.

While the two cores in the north central Pacific, NGC55 and NP18, show similar long-term trends of $^{87}Sr/^{86}Sr$ ratio, the third core NP29 in the east of the Mariana arc has different features. In fact, continental and volcanic fluxes of NP29 show a different fluctuation pattern from those of NGC55 and NP18 (Fig. 5). The continental and volcanic fluxes both decrease during the past 3 my. A drop in Sr isotopic ratio of NP29 at 1.9 Ma is caused by a decreased input of the continental material. From 1.9 to 0.8 Ma, the $^{87}Sr/^{86}Sr$ ratio of NP29 increases due to a reduced volcanic supply, not due to an increase of the eolian material. NP29 is in close vicinity to Mariana Islands, Magellan Seamounts and Marshall

Islands. Their volcanic supply to the area of NP29 may have fluctuated. Moreover, there is a possibility that the current of the middle-latitude westerlies was not influential in the area of NP29 and that the supply of the continental material did not increase there. This may be related to the hiatus between 1.5 Ma and the present in the core NP27 (19° 59.88 N, 158° 29.87 E, 5582 m; [16]) that is close to NP29.

The $^{87}Sr/^{86}Sr$ ratios of all three sites start to decrease synchronously from around 0.8 Ma to the present. The decrease is caused by a reduced supply of the Asian continental material to the north Pacific (Fig. 5). This is supported by the mass-accumulation rates of north Pacific pelagic clays at DSDP Site 578 [32], at LL44-GPC-3 [33] and at KK75-02 [34] that show decreased supplies of the continental material during that period. The age of 0.8 Ma may relate to the middle Pleistocene shift which is the change in the nature of fluctuations from the early to the late Pleistocene [27, 35]. The aridity associated with loess formation in the Asia may have changed, although the linkage is not clear.

The $^{87}Sr/^{86}Sr$ variations in the detrital sediments inversely correlate with the variations of magnetic susceptibility reported for all cores examined here (Figs. 2-a, b and c; [5, 17]). Yamazaki and Ioka [5] suggest that magnetic minerals of pelagic clay in the north Pacific consist predominantly of two components: one is detrital hematite and magnetite (and/or maghemite) transported as eolian dust and the other is biogenic magnetite formed in situ. Biogenic magnetite is produced in the surface sediments at a constant rate and has high susceptibility. When the continental component with a high $^{87}Sr/^{86}Sr$ ratio and a low susceptibility comes to be dominant in sediments, the ratio becomes high and the susceptibility becomes low. The variations of Sr isotopic ratio and magnetic susceptibility in pelagic sediments are both considered to reflect changes in eolian flux from arid regions in the Asia.

5.2 Cyclic change of $^{87}Sr/^{86}Sr$ ratio

Despite the difference of sedimentation localities, the Sr isotopic variations in all three cores have fluctuation patterns fairly similar to each other. They show similar cyclic changes (Figs. 2-a, b and c). For example, all the cores have lower $^{87}Sr/^{86}Sr$ ratios at about 0.1, 0.5 and 1.7-1.9 Ma and higher ratios at about 0.3, 0.8, 1.6, 2.0 and 2.3-2.4 Ma.

The frequency spectrum of the $^{87}Sr/^{86}Sr$ record was examined and compared to the periodicities of the earth's orbital parameters as estimated by Berger [36]. Data from 0 to 2.58 Ma, that is the Quaternary, were used in this spectral analysis. Two data of NP18 at 2.526 Ma and 2.562 Ma, which are anomalously low $^{87}Sr/^{86}Sr$ ratios, were not used. The data used for this spectral analysis were interpolated from the raw data by spline function. The long-term trend during the Quaternary was removed by subtraction of a 3rd order polynomial fit to $^{87}Sr/^{86}Sr$ data. Autocorrelation of the data, smoothing with a Bartlett window and Blackman-Turkey method were conducted using the time-series analysis of Paillard et al. [37]. Cross-spectral analysis was also used to compare the $^{87}Sr/^{86}Sr$ records with the eccentricity of the earth's orbit and to assess directly the coherency at each frequency.

Variance spectra of NGC55, NP18 and NP29 cores and the eccentricity of the earth's orbit together with their coherency spectra are shown in Fig. 6. Temporal resolution of $^{87}Sr/^{86}Sr$ record, 17 - 40 ky as mentioned in the above section, prevents the detection of the short periodicities associated with tilt and precession (< 50 ky; [36]) and, therefore, only the eccentricity is used for this comparison. Spectral analyses of the three $^{87}Sr/^{86}Sr$ time series spanning the Quaternary show that the record of NP29 is strongly influenced by the 400 ky periodicity and that those of NGC55 and NP18 are also influenced by the same periodicity. Among the periodicities of the Milankovitch Cycle associated with the eccentricity of the earth's

orbit, 100 ky (126 and 96 ky) and 412 ky periodicities are important [36]. For all the cores, the $^{87}Sr/^{86}Sr$ record and the eccentricity are highly coherent at the 400 ky earth-orbital period (Fig. 6).

The $^{87}Sr/^{86}Sr$ variation in NGC55, the core with the highest sedimentation rate among the three cores, is compared with the SPECMAP stacked $\delta^{18}O$ record [38] for the period from 0.8 Ma to the present. The SPECMAP stack is a well-established climate indicator. It is found that the $^{87}Sr/^{86}Sr$ variation is remarkably similar to the variation of $\delta^{18}O$ (Fig. 7). Higher ratios correspond well with glacial periods (even numbers in Fig. 7) and lower ones correspond well with interglacial periods. The variance spectrum of the $^{87}Sr/^{86}Sr$ record of NGC55 is concentrated at approximately 100 ky and the $^{87}Sr/^{86}Sr$ record and the eccentricity of the earth's orbit are coherent at about 100 ky (Fig. 6). Fine structure of the glacial-interglacial cycle appears to be superimposed on the main structure of increasing and decreasing trends and the fluctuation of the 400 ky periodicity discussed above. Some small time lags between the $^{87}Sr/^{86}Sr$ ratio fluctuation and the $\delta^{18}O$ curve (Fig. 7) may be caused by the inaccurate assumption of linear sedimentation rates between boundaries of geomagnetic reversals. While the NGC55 core has a relatively high sedimentation rate (0.10 g cm^{-2} ky^{-1}), the NP18 and the NP29 cores have small sedimentation rates (< 0.05 g cm^{-2} ky^{-1}) during the past 0.8 my. Their small sedimentation rates are likely to have prevented shorter periodicities in $^{87}Sr/^{86}Sr$ variation according to the Milankovitch Cycle.

The $^{87}Sr/^{86}Sr$ ratios in north Pacific sediment depend on the share of the continental component from east Asia. If volcanic supply is constant, the glacial-interglacial cycle of $^{87}Sr/^{86}Sr$ variation in the pelagic sediments is considered to be controlled by the load of eolian input with a high $^{87}Sr/^{86}Sr$ ratio of the Asian continental signature. Actually, periods of higher

$^{87}Sr/^{86}Sr$ ratio tend to be longer than those of lower ratio on the diagram and this fluctuation pattern suggests a reflection of the eolian flux with the high $^{87}Sr/^{86}Sr$ ratio (Fig. 7). The northern hemisphere was more arid and more dust was transported during glacial periods than during interglacial periods [39]. The cycle of the $^{87}Sr/^{86}Sr$ ratio must correspond to the paleoclimatic cycle of the aridity in the Asian continent [40].

6. Conclusions

The temporal variation of Sr isotopes in the detrital component of the north Pacific sediment was precisely examined. The north Pacific sediments are mixtures of the Asian continental material with a high $^{87}Sr/^{86}Sr$ ratio (0.724 - 0.726) and volcanic material with a low ratio (0.703 - 0.705). Assuming that the volcanic flux is constant, the temporal variation in Sr isotopic composition of pelagic sediment in the north Pacific indicates the eolian flux from the continent.

1. The $^{87}Sr/^{86}Sr$ ratio in the north central Pacific sediment increases over the period from 3 to 0.8 Ma. This reflects an increased eolian input from the arid region in the Asian continent, which must be related to aridification of the continent.

2. The decreasing $^{87}Sr/^{86}Sr$ ratio in the north Pacific sediment during the past 0.8 my implies a decreasing eolian flux. The age of 0.8 Ma may be related to the climatic event known as the middle Pleistocene shift.

3. The $^{87}Sr/^{86}Sr$ variations in the detrital sediments inversely correlate with the variations of magnetic susceptibility. The variations of $^{87}Sr/^{86}Sr$ ratio and magnetic susceptibility in detrital sediments are both considered to reflect changes in eolian flux from the Asian continent.

4. $^{87}Sr/^{86}Sr$ records show cyclic fluctuations with periodicities of 400 ky and 100 ky

which are associated with the eccentricity of the earth's orbit (Milankovitch Cycle). This must reflect a fluctuation of the eolian flux corresponding to the aridity in the Asian continent.

$^{87}Sr/^{86}Sr$ variation as shown here is expected to exist in any pelagic and hemi-pelagic sediments in the north Pacific. Precise and sequential analyses of radiogenic isotopes for detrital sediments may reveal changes of the aridity of source regions in the Asian continent, volcanic supply and atmospheric circulation.

Acknowledgements

I thank the members of the Department of Earth and Planetary Sciences, Nagoya University, and Geological Survey of Japan (GSJ). I especially wish to express my gratitude to Professor T. Tanaka, Nagoya University, who continually contributed with suggestions and criticism and to Dr. A. Nishimura and Dr. T. Yamazaki, GSJ, who provided the samples and contributed with suggestion. I also thank Dr. H. Kamioka for performing the isotope analysis at GSJ; Professor S. Nakai, University of Tokyo, for valuable discussion; and Professors. I. Kawabe and K. Yamamoto and Dr. K. Mimura, Nagoya University, for encouragement. I am indebted to Dr. C. Dragusanu, Hiroshima University, and Dr. C. Richardson, University of Cambridge, for their patience in revising the English version of this paper. Part of this work represents a Northwest Pacific Carbon Cycle (NOPACC) study assigned to the Kansai Environmental Engineering Center (KEEC) by the New Energy and Industrial Technology Development Organization (NEDO) and special program of the Ministry of International Trade and Industry (MITI) for studying element cycles in the ocean.

References

[1] M. E. Raymo, W. F. Ruddiman, N. J. Shackleton and D. W. Oppo, Evolution of Atlantic - Pacific $\delta^{13}C$ gradients over the last 2.5 m.y., Earth Planet. Sci. Lett. 97, 353-368, 1990.

[2] T. C. Moore, Jr., N. G. Pisias and D. A. Dunn, Carbonate time series of the Quaternary and Late Miocene sediments in the Pacific Ocean: A spectral comparison, Mar. Geol. 46, 217-233, 1982.

[3] J. Bloemendal and P. deMenocal, Evidence for a change in the periodicity of tropical climate cycles at 2.4 Myr from whole-core magnetic susceptibility measurements, Nature 342, 897-900, 1989.

[4] T. Yamazaki and N. Ioka, Long-term secular variation of the geomagnetic field during the last 200 kyr recorded in sediment cores from the western equatorial Pacific, Earth Planet. Sci. Lett. 128, 527-544, 1994.

[5] T. Yamazaki and N. Ioka, Environmental rock-magnetism of pelagic clay: Implications for Asian eolian input to the North Pacific since the Pliocene, Paleoceanography 12, 111-124, 1997.

[6] M. Parra, J. -C. Faugères, F. Grousset and C. Pujol, Sr-Nd isotopes as tracers of fine-grained detrital sediments: the South-Barbados accretionary prism during the last 150 kyr, Mar. Geol. 136, 225-243, 1997.

[7] M. Revel, M. Cremer, F. E. Grousset and L. Labeyrie, Grain-size and Sr-Nd isotopes as tracer of paleo-bottom current strength, Northeast Atlantic Ocean, Mar. Geol. 131, 233-249, 1996.

[8] M. Revel, J. A. Sinko and F. E. Grousset, Sr and Nd isotopes as tracers of North

Atlantic lithic particles: Paleoclimatic implications, Paleoceanography 11, 95-113, 1996.

[9] E. J. Dasch, Strontium isotopes in weathering profiles, deep-sea sediments, and sedimentary rocks, Geochim. Cosmochim. Acta 33, 1521-1552, 1969.

[10] P. E. Biscaye, R. Chesselet and J. M. Prospero, Rb-Sr, $^{87}Sr/^{86}Sr$ isotope system as an index of provenance of continental dusts in the open Atlantic Ocean, J. Rech. Atmos. 8, 819-829, 1974.

[11] F. E. Grousset, P. E. Biscaye, A. Zindler, J. Prospero and R. Chester, Neodymium isotopes as tracers in marine sediments and aerosols: North Atlantic, Earth Planet. Sci. Lett. 87, 367-378, 1988.

[12] Y. Asahara, T. Tanaka, H. Kamioka and A. Nishimura, Asian continental nature of $^{87}Sr/^{86}Sr$ ratios in north central Pacific sediments, Earth Planet. Sci. Lett. 133, 105-116, 1995.

[13] S. Nakai, A. N. Halliday and D. K. Rea, Provenance of dust in the Pacific Ocean, Earth Planet. Sci. Lett. 119, 143-157, 1993.

[14] P. E. Biscaye, F. E. Grousset, M. Revel, S. Van der Gaast, G. A. Zielinski, A. Vaars, G. Kukla, Asian provenance of glacial dust (stage 2) in the Greenland Ice Sheet Project 2 Ice Core, Summit, Greenland, J. Geophys. Res. 102, 26765-26781, 1997.

[15] Y. Tanaka, K. Ikehara and J. Suzuki, Deep-sea sediments along the 175°E longitude and Hess Rise, 1994FY report on 'Study on Element Cycles in Ocean', Geol. Surv. Jpn., pp. 68-79, 1995 (in Japanese).

[16] K. Ikehara and A. Nishimura, Deep-sea sediments along the 20°N transect from Hawaii to Mariana and in the West Caroline Basin, 1992FY report on 'Marine Geological Study on Element Cycles in Ocean', Geol. Surv. Jpn., pp. 51-66, 1993 (in Japanese).

[17] T. Yamazaki, Rock magnetism and paleomagnetism of sediments at 20°N from west of Hawaii to east of Mariana, 1992FY report on 'Marine Geological Study on Element Cycles in Ocean', Geol. Surv. Jpn., pp. 82-98, 1993 (in Japanese).

[18] W. A. Berggren, F. J. Hilgen, C. G. Langereis, D. V. Kent, J. D. Obradovich, I. Raffi, M. E. Raymo and N. J. Shackleton, Late Neogene chronology: New perspectives in high-resolution stratigraphy, GSA Bull. 107, 1272-1287, 1995.

[19] K. Ikehara and A. Nishimura, Physical properties of sediments along the 20°N transect from Hawaii to Mariana and in the West Caroline Basin, 1992FY report on 'Marine Geological Study on Element Cycles in Ocean', Geol. Surv. Jpn., pp. 67-74, 1993 (in Japanese).

[20] K. Ikehara and I. Motoyama, Physical properties of deep-sea sediments along the 175°E longitude and Hess Rise, 1994FY report on 'Study on Element Cycles in Ocean', Geol. Surv. Jpn., pp. 80-99, 1995 (in Japanese).

[21] Y. Asahara, T. Tanaka, H. Kamioka, A. Nishimura and T. Yamazaki, Provenance of the north Pacific sediments and process of source material transport as derived from Rb-Sr isotopic systematics, Chem. Geol. 159, 1999.

[22] C. E. Hedge and F. G. Walthall, Radiogenic strontium-87 as an index of geologic processes, Science 140, 1214-1217, 1963.

[23] H. Kurasawa, Isotopic composition of strontium in volcanic rocks from Fuji, Hakone and Izu area, Central Japan, Bull. Volcanol. Soc. Jpn. 24, 135-152, 1979 (in Japanese with English Abstr.).

[24] S. Nohda and G. J. Wasserburg, Nd and Sr isotopic study of volcanic rocks from Japan, Earth Planet. Sci. Lett. 52, 264-276, 1981.

[25] K. Notsu, N. Isshiki and M. Hirano, Comprehensive strontium isotope study of Quaternary volcanic rocks from the Izu-Ogasawara arc, Geochem. J. 17, 289-302, 1983.

[26] S. J. Goldstein and S. B. Jacobsen, Nd and Sr isotopic systematics of river water suspended material: implications for crustal evolution, Earth Planet. Sci. Lett. 87, 249-265, 1988.

[27] W. F. Ruddiman and M. E. Raymo, Northern Hemisphere climate régimes during the past 3 Ma: possible tectonic connections, in: The past three million years: Evolution of climatic variability in the north Atlantic region, N. J. Shackleton, R. G. West and D. Q. Bowen, eds., pp. 411-430, Phil. Trans. R. Soc. Lond. B318, London, 1988.

[28] N. J. Shackleton, J. Backman, H. Zimmerman, D. V. Kent, M. A. Hall, D. G. Roberts, D. Schnitker, J. G. Baldauf, A. Desprairies, R. Homrighausen, P. Huddlestun, J. B. Keene, A. J. Kaltenback, K. A. O. Krumsiek, A. C. Morton, J. W. Murray and J. Westberg-Smith, Oxygen isotope calibration of the onset of ice-rafting and history of glaciation in the North Atlantic region, Nature 307, 620-623, 1984.

[29] D. K. Rea, I. A. Basov, L. A. Krissek and the Leg 145 Scientific Party, Scientific results of drilling the North Pacific Transect, Proc. Ocean Drill. Program Sci. Results 145, 577-596, 1995.

[30] F. Heller and T. S. Liu, Magnetostratigraphical dating of loess deposits in China, Nature 300, 431-433, 1982.

[31] F. Heller and T. S. Liu, Magnetism of Chinese loess deposits, Geophys. J. R. Astron. Soc. 77, 125-141, 1984.

[32] T. R. Janecek, Eolian sedimentation in the northwest Pacific Ocean: Preliminary examination of the data from Deep Sea Drilling Project Sites 576 and 578, Initial Rep.

Deep Sea Drill. Proj. 86, 589-603, 1985.

[33] D. K. Rea and T. R. Janecek, Late Cenozoic changes in atmospheric circulation deduced from North Pacific eolian sediments, Mar. Geol. 49, 149-167, 1982.

[34] D. K. Rea, M. Leinen and T. R. Janecek, Geologic approach the long-term history of atmospheric circulation, Science 227, 721-725, 1985.

[35] W. H. Berger, M. K. Yasuda, T. Bickert, G. Wefer and T. Takayama, Quaternary time scale for the Ontong Java Plateau: Milankovitch template for Ocean Drilling Program Site 806, Geology 22, 463-467, 1994.

[36] A. Berger, Milankovitch theory and climate, Rev. Geophys. 26, 624-657, 1988.

[37] D. Paillard, L. Labeyrie and P. Yiou, Macintosh program performs time-series analysis, Eos Trans. AGU 77, 379, 1996.

[38] J. Imbrie, J. D. Hays, D. G. Martinson, A. McIntyre, A. C. Mix, J. J. Morley, N. G. Pisias, W. L. Prell and N. J. Shackleton, The orbital theory of Pleistocene climate: support from a revised chronology of the Marine $\delta^{18}O$ record, in: Milankovitch and Climate, Part 1, A. Berger, J. Imbrie, J. Hays, G. Kukla and B. Saltzman, eds., pp. 269-305, Reidel, Dordrecht, 1984.

[39] D. K. Rea, The paleoclimatic record provided by eolian deposition in the deep sea: the geologic history of wind, Rev. Geophys. 32, 159-195, 1994.

[40] G. Kukla and Z. An, Loess stratigraphy in central China, Paleogeogr. Paleoclimatol. Paleoecol. 72, 203-225, 1989.

FIGURE CAPTIONS

Fig. 1 Locations of NGC55, NP18 and NP29 cores on the distribution map of Sr isotopic compositions in the Pacific surface sediments from Asahara et al. [12]. Open circles are locations of surface sediments in the previous study. Stars are locations of the core samples in this study.

Fig. 2 Temporal variations of $^{87}Sr/^{86}Sr$ ratio and magnetic susceptibility of core NGC55 (a), NP18 (b) and NP29 (c). They correlate inversely. Data of magnetic susceptibility is from Yamazaki and Ioka [5] and Yamazaki [17]. Note that scale of magnetic susceptibility is inverted. The horizontal bars at the top of diagrams show the geomagnetic polarity intervals (black / white shows normal / reversed polarity).

Fig. 3 Temporal variation in Sr isotopic ratio and accumulation rate of the three core samples. Thick lines show Sr isotopic ratios and thin lines show accumulation rates. Averages of Sr isotopic ratio and accumulation rate in each geomagnetic polarity interval are shown.

Fig. 4 Rb-Sr isochron plot for the detrital components in the three core samples of the north Pacific sediments and in three size fractions of the Asian continental materials (loess and river deposit). These data are from Asahara et al. [21]. The Rb-Sr isotopic systematics of the core sediments show a well-correlated pseudo isochron. This pseudo isochron reflects the mixing of two material, i.e., the Asian continental material with high

$^{87}Rb/^{86}Sr$ ratios (5.0 - 6.0) and high $^{87}Sr/^{86}Sr$ ratios (0.724 - 0.726) and the volcanic material with low $^{87}Rb/^{86}Sr$ ratios (0.0 - 0.1) and low $^{87}Sr/^{86}Sr$ ratios (0.703 - 0.705), from island-arc volcanics such as the Izu-Ogasawara-Mariana arc and oceanic islands such as the Hawaiian Islands. Continental component of the core sediments has a high $^{87}Rb/^{86}Sr$ ratio that implies fine particles (a few μm) transported from the Asian continent by wind. Data field for volcanic material [22-25] and riverine suspended material in the Japanese Islands [26] are shown on this diagram.

Fig. 5 Temporal variation of fluxes of the continental and volcanic materials in each core [21]. Fluxes are calculated from the relative amounts of the continental and the volcanic fluxes and sedimentation rate (Fig. 3). The continental flux corresponds to the eolian flux from the Asian continent. The data at 0.83 Ma of NP18 (dotted line) is excluded because sedimentation rate at 0.83 Ma may not be correct.

Fig. 6 Variance spectra of Sr isotopic ratio of NGC55, NP18 and NP29 cores and the eccentricity of the earth's orbit and coherency spectra between Sr isotopic ratios and the eccentricity. The significance level (80%) is shown. The long-term trend during the Quaternary is removed by subtraction of a 3rd order polynomial fit to $^{87}Sr/^{86}Sr$ data before spectral analysis. High concentrations of variance spectra of the eccentricity (0.412, 0.126 and 0.096 my) are shown. The $^{87}Sr/^{86}Sr$ records and the eccentricity have high coherencies at the 400 ky earth-orbital (Milankovitch) period.

Fig. 7 Comparison between the $^{87}Sr/^{86}Sr$ record of the NGC55 core and the SPECMAP

stacked $\delta^{18}O$ record [38]. Oxygen isotopic stages are labelled. Even numbers represent glacial periods. High frequencies of the $^{87}Sr/^{86}Sr$ variation are remarkably similar to the $\delta^{18}O$ curve.

Table 1

Sample descriptions

Core sample	Location		Depth (m)	Description	ref.[a]	Sample of surface sediment in close proximity to the core sample and its $^{87}Sr/^{86}Sr$ ratio [b]	
	Latitude	Longitude					
NGC55	24° 00.14'N	175° 06.56'E	5741	Core length 362 cm, dark brown to brown clay.	[5, 15]	NB69	0.719086
NP18	20° 00.03'N	175° 07.11'W	5323	Core length 676 cm, brown to dark brown clay.	[5, 16]	NB37	0.718812
NP29	19° 59.92'N	153° 28.91'E	5262	Core length 700 cm, brown to dark brown clay. Ferromangnese nodules occur at depths of 0.30 and 1.93 m.	[16]	NB50	0.712928

a Data sources for sample descriptions.
b Data source is Asahara et al. [12].

Table 2
Sr isotopic data for NGC55, NP18 and NP29 cores

depth(cm)	age(Ma)	$^{87}Sr/^{86}Sr$ *	depth(cm)	age(Ma)	$^{87}Sr/^{86}Sr$ *	depth(cm)	age(Ma)	$^{87}Sr/^{86}Sr$ *
NGC55			98 - 99	0.718	0.719763±13	218 - 219	1.701	0.719241±16
0 - 1	0.004	0.719219±14	100 - 101	0.733	0.719796±16	220 - 221	1.717	0.719389±13
1 - 2	0.011	0.718827±17	102 - 103	0.747	0.719647±14	222 - 223	1.733	0.719091±16
2 - 3	0.018	0.718889±14	104 - 105	0.762	0.719839±14	224 - 225	1.750	0.719003±14
3 - 4	0.026	0.719094±16	106 - 107	0.776	0.719813±14	226 - 227	1.766	0.718970±14
4 - 5	0.033	0.719083±14	108 - 109	0.791	0.719863±16	228 - 229	1.797	0.719095±14
5 - 6	0.040	0.718962±14	110 - 111	0.805	0.719880±16	230 - 231	1.833	0.719055±17
6 - 7	0.047	0.719103±14	112 - 113	0.820	0.719778±14	232 - 233	1.869	0.719076±14
7 - 8	0.055	0.719272±16	114 - 115	0.834	0.719905±17	234 - 235	1.905	0.719027±16
8 - 9	0.062	0.719319±14	116 - 117	0.849	0.719981±17	236 - 237	1.941	0.719082±14
9 - 10	0.069	0.719309±14	118 - 119	0.863	0.719973±16	238 - 239	1.964	0.719139±14
10 - 11	0.077	0.719290±16	120 - 121	0.878	0.719937±16	240 - 241	1.982	0.719223±14
11 - 12	0.084	0.719282±16	122 - 123	0.892	0.719832±16	242 - 243	2.001	0.719280±14
12 - 13	0.091	0.719289±17	124 - 125	0.907	0.719669±14	244 - 245	2.019	0.718783±14
13 - 14	0.098	0.719229±16	126 - 127	0.921	0.719705±14	246 - 247	2.038	0.718869±17
14 - 15	0.106	0.719297±16	128 - 129	0.936	0.719878±16	248 - 249	2.057	0.718844±16
15 - 16	0.113	0.719310±16	130 - 131	0.950	0.719829±17	250 - 251	2.075	0.718782±14
16 - 17	0.120	0.719187±16	132 - 133	0.965	0.719791±14	252 - 253	2.094	0.718757±16
17 - 18	0.128	0.719217±14	134 - 135	0.979	0.719836±16	254 - 255	2.112	0.718928±17
18 - 19	0.135	0.719166±14	136 - 137	0.998	0.719793±14	256 - 257	2.131	0.718923±13
19 - 20	0.142	0.719352±14	138 - 139	1.030	0.719766±16	258 - 259	2.149	0.718724±16
20 - 21	0.149	0.719353±14	140 - 141	1.062	0.719699±14	260 - 261	2.168	0.718695±14
22 - 23	0.164	0.719280±14	142 - 143	1.082	0.719686±14	262 - 263	2.186	0.718822±17
24 - 25	0.179	0.719396±16	144 - 145	1.098	0.719758±16	264 - 265	2.205	0.718644±14
26 - 27	0.193	0.719332±16	146 - 147	1.115	0.719491±14	266 - 267	2.223	0.718629±16
28 - 29	0.208	0.719363±14	148 - 149	1.131	0.719577±16	268 - 269	2.242	0.718665±14
30 - 31	0.222	0.719359±14	150 - 151	1.147	0.719671±14	270 - 271	2.260	0.718764±13
32 - 33	0.237	0.719478±14	152 - 153	1.164	0.719536±16	272 - 273	2.279	0.718663±16
34 - 35	0.251	0.719547±14	154 - 155	1.180	0.719546±14	274 - 275	2.297	0.718748±16
36 - 37	0.266	0.719391±14	156 - 157	1.196	0.719396±13	276 - 277	2.316	0.718845±13
38 - 39	0.281	0.719430±17	158 - 159	1.212	0.719586±16	278 - 279	2.334	0.718954±16
40 - 41	0.295	0.719540±16	160 - 161	1.229	0.719712±14	280 - 281	2.353	0.718726±14
42 - 43	0.310	0.719538±14	162 - 163	1.245	0.719744±14	282 - 283	2.372	0.718754±16
44 - 45	0.324	0.719462±14	164 - 165	1.261	0.719654±16	284 - 285	2.390	0.718922±14
46 - 47	0.339	0.719427±14	166 - 167	1.278	0.719671±17	286 - 287	2.409	0.719320±14
48 - 49	0.354	0.719418±14	168 - 169	1.294	0.719655±16	288 - 289	2.427	0.719052±14
50 - 51	0.368	0.719577±17	170 - 171	1.310	0.719576±14	290 - 291	2.446	0.718642±14
52 - 53	0.383	0.719642±16	172 - 173	1.326	0.719738±13	292 - 293	2.464	0.718510±16
54 - 55	0.397	0.719394±14	174 - 175	1.343	0.719573±14	294 - 295	2.483	0.718536±16
56 - 57	0.412	0.719282±17	176 - 177	1.359	0.719458±14	296 - 297	2.501	0.718576±14
58 - 59	0.426	0.719160±16	178 - 179	1.375	0.719624±14	298 - 299	2.520	0.718492±13
60 - 61	0.441	0.719328±16	180 - 181	1.392	0.719547±16	300 - 301	2.538	0.718544±13
62 - 63	0.456	0.719417±13	182 - 183	1.408	0.719458±17	301 - 302	2.548	0.718457±16
64 - 65	0.470	0.719431±17	184 - 185	1.424	0.719595±14	302 - 303	2.557	0.718417±16
66 - 67	0.485	0.719272±14	186 - 187	1.440	0.719380±14	303 - 304	2.566	0.718543±14
68 - 69	0.499	0.719231±14	188 - 189	1.457	0.719206±16	304 - 305	2.575	0.718491±14
70 - 71	0.514	0.719246±14	190 - 191	1.473	0.719232±17	305 - 306	2.585	0.718454±13
72 - 73	0.529	0.719287±13	192 - 193	1.489	0.719288±16	306 - 307	2.594	0.718393±16
74 - 75	0.543	0.719321±14	194 - 195	1.505	0.719344±13	307 - 308	2.603	0.718446±14
76 - 77	0.558	0.719473±16	196 - 197	1.522	0.719351±14	308 - 309	2.612	0.718183±13
78 - 79	0.572	0.719342±16	198 - 199	1.538	0.719349±14	309 - 310	2.622	0.718059±16
80 - 81	0.587	0.719325±14	200 - 201	1.554	0.719065±13	310 - 311	2.631	0.718079±14
82 - 83	0.601	0.719468±17	202 - 203	1.571	0.719330±14	312 - 313	2.649	0.717809±14
84 - 85	0.616	0.719521±14	204 - 205	1.587	0.719314±14	314 - 315	2.668	0.718067±14
86 - 87	0.631	0.719711±14	206 - 207	1.603	0.719353±17	316 - 317	2.687	0.717980±16
88 - 89	0.645	0.719690±14	208 - 209	1.619	0.719612±17	318 - 319	2.705	0.718252±14
90 - 91	0.660	0.719891±16	210 - 211	1.636	0.719565±14	320 - 321	2.724	0.718133±13
92 - 93	0.674	0.719804±14	212 - 213	1.652	0.719487±14	322 - 323	2.742	0.718169±16
94 - 95	0.689	0.719518±17	214 - 215	1.668	0.719516±14	324 - 325	2.761	0.718065±14
96 - 97	0.703	0.719760±13	216 - 217	1.685	0.719277±17	326 - 327	2.779	0.717933±16

Table 2 (continued)

depth(cm)	age(Ma)	$^{87}Sr/^{86}Sr$ *	depth(cm)	age(Ma)	$^{87}Sr/^{86}Sr$ *	depth(cm)	age(Ma)	$^{87}Sr/^{86}Sr$ *
NGC55			80 - 81	1.495	0.719162±13	280 - 281		0.714988±16
328 - 329	2.798	0.717713±13	82 - 83	1.532	0.719261±14	290 - 291		0.714658±16
330 - 331	2.816	0.717574±16	84 - 85	1.569	0.719325±16	300 - 301		0.714548±12
332 - 333	2.835	0.717737±13	86 - 87	1.606	0.719109±13	310 - 311		0.714472±14
334 - 335	2.853	0.717737±17	88 - 89	1.643	0.719109±13	320 - 321		0.713667±16
336 - 337	2.872	0.717867±17	90 - 91	1.679	0.718948±12	330 - 331		0.713461±14
338 - 339	2.890	0.717962±13	92 - 93	1.716	0.718414±13	340 - 341		0.713028±14
340 - 341	2.909	0.717864±14	94 - 95	1.753	0.717989±14	350 - 351		0.713254±17
342 - 343	2.927	0.717507±14	96 - 97	1.788	0.718362±14	360 - 361		0.713003±14
344 - 345	2.946	0.717848±16	98 - 99	1.821	0.718544±14	370 - 371		0.713206±16
346 - 347	2.964	0.717739±16	100 - 101	1.854	0.718533±13	380 - 381		0.712919±14
348 - 349	2.983	0.717323±14	102 - 103	1.887	0.718677±13	390 - 391		0.712863±17
350 - 351	3.002	0.717673±14	104 - 105	1.920	0.718800±14	400 - 401		0.712701±16
352 - 353	3.020	0.717421±14	106 - 107	1.954	0.718762±12	410 - 411		0.712683±17
354 - 355	3.039	0.717644±14	108 - 109	1.989	0.718568±13			
356 - 357	3.057	0.717741±13	110 - 111	2.025	0.718553±11	NP29		
358 - 359	3.076	0.717574±16	112 - 113	2.061	0.718466±11	0 - 1	0.013	0.714174±16
360 - 361	3.094	0.717433±14	114 - 115	2.097	0.718465±11	2 - 3	0.067	0.714119±16
			116 - 117	2.133	0.718554±11	4 - 5	0.120	0.714123±14
NP18			118 - 119	2.168	0.718463±11	6 - 7	0.173	0.714126±14
0 - 1	0.008	0.718851±14	120 - 121	2.204	0.718442±11	8 - 9	0.226	0.715154±14
2 - 3	0.041	0.718799±12	122 - 123	2.240	0.718332±11	10 - 11	0.280	0.714927±14
4 - 5	0.074	0.718816±12	124 - 125	2.276	0.718409±13	12 - 13	0.333	0.714865±14
6 - 7	0.107	0.718881±10	126 - 127	2.312	0.718201±13	14 - 15	0.386	0.715009±14
8 - 9	0.140	0.718815±16	128 - 129	2.347	0.718342±14	16 - 17	0.439	0.714884±14
10 - 11	0.173	0.719281±12	130 - 131	2.383	0.717756±11	18 - 19	0.492	0.714791±16
12 - 13	0.206	0.719100±12	132 - 133	2.419	0.717329±14	20 - 21	0.546	0.715574±16
14 - 15	0.239	0.719306±13	134 - 135	2.455	0.717379±13	22 - 23	0.599	0.715499±14
16 - 17	0.272	0.719197±13	136 - 137	2.491	0.716488±13	24 - 25	0.652	0.715645±14
18 - 19	0.305	0.719444±14	138 - 139	2.526	0.714732±16	26 - 27	0.705	0.715709±14
20 - 21	0.338	0.719275±12	140 - 141	2.562	0.713168±14	28 - 29	0.759	0.715435±16
22 - 23	0.371	0.719250±12	142 - 143	2.609	0.717380±16	30 - 31	0.804	0.715468±16
24 - 25	0.404	0.719255±39	144 - 145	2.667	0.717203±14	32 - 33	0.843	0.716055±16
26 - 27	0.437	0.719184±12	146 - 147	2.725	0.717320±10	34 - 35	0.882	0.715833±14
28 - 29	0.470	0.719038±12	148 - 149	2.783	0.716920±13	36 - 37	0.921	0.715174±16
30 - 31	0.503	0.718992±13	150 - 151	2.841	0.716981±13	38 - 39	0.961	0.714970±14
32 - 33	0.536	0.718979±13	152 - 153	2.899	0.717056±11	40 - 41	0.997	0.715088±13
34 - 35	0.569	0.719364±16	154 - 155	2.957	0.716855±16	42 - 43	1.025	0.715293±14
36 - 37	0.602	0.719381±30	156 - 157	3.015	0.717092±11	44 - 45	1.053	0.715166±13
38 - 39	0.635	0.719393±13	158 - 159	3.073	0.717087±11	46 - 47	1.081	0.714771±16
40 - 41	0.668	0.719295±12	160 - 161	3.131	0.717263±19	48 - 49	1.109	0.714608±16
42 - 43	0.701	0.719491±13	162 - 163	3.189	0.717489±22	50 - 51	1.136	0.715207±16
44 - 45	0.734	0.719690±13	164 - 165	3.247	0.717148±17	52 - 53	1.164	0.715261±16
46 - 47	0.767	0.719500±13	166 - 167	3.305	0.717115±20	54 - 55	1.191	0.715748±16
48 - 49	0.830	0.719728±14	168 - 169	3.363	0.717063±19	56 - 57	1.219	0.715966±14
50 - 51	0.914	0.719668±12	170 - 171	3.421	0.716644±11	58 - 59	1.246	0.715394±14
52 - 53	0.993	0.719621±13	172 - 173	3.479	0.716933±16	60 - 61	1.274	0.714796±14
54 - 55	1.024	0.719625±13	174 - 175	3.537	0.716815±17	62 - 63	1.301	0.715051±16
56 - 57	1.055	0.719667±13	176 - 177		0.716789±29	64 - 65	1.329	0.714976±14
58 - 59	1.088	0.719557±13	178 - 179		0.716811±17	66 - 67	1.356	0.714973±16
60 - 61	1.125	0.719335±14	180 - 181		0.716313±13	68 - 69	1.384	0.714505±13
62 - 63	1.162	0.719506±14	190 - 191		0.716753±11	70 - 71	1.411	0.715196±14
64 - 65	1.199	0.719180±10	200 - 201		0.716662±14	72 - 73	1.439	0.714816±14
66 - 67	1.236	0.719291±13	210 - 211		0.716272±11	74 - 75	1.466	0.714847±14
68 - 69	1.273	0.719107±14	220 - 221		0.716059±13	76 - 77	1.494	0.714245±14
70 - 71	1.310	0.719058±13	230 - 231		0.716051±11	78 - 79	1.521	0.714029±16
72 - 73	1.347	0.718966±23	240 - 241		0.715983±13	80 - 81	1.549	0.714362±14
74 - 75	1.384	0.719146±14	250 - 251		0.715611±11	82 - 83	1.576	0.714571±14
76 - 77	1.421	0.719271±13	260 - 261		0.715363±17	84 - 85	1.604	0.715050±14
78 - 79	1.458	0.719141±12	270 - 271		0.715385±17	86 - 87	1.631	0.715910±16

Table 2 (continued)

depth(cm)	age(Ma)	$^{87}Sr/^{86}Sr$ *	depth(cm)	age(Ma)	$^{87}Sr/^{86}Sr$ *	depth(cm)	age(Ma)	$^{87}Sr/^{86}Sr$ *
NP29			194 - 195	2.693	0.715537±14	302 - 303	3.531	0.714884±13
88 - 89	1.659	0.715900±14	196 - 197	2.708	0.715484±14	304 - 305	3.543	0.714851±13
90 - 91	1.686	0.715896±16	198 - 199	2.722	0.715335±14	306 - 307	3.555	0.714809±16
92 - 93	1.714	0.715785±16	200 - 201	2.737	0.714838±16	308 - 309	3.567	0.714733±14
94 - 95	1.741	0.715748±16	202 - 203	2.752	0.714987±14	310 - 311	3.579	0.714730±16
96 - 97	1.769	0.715670±16	204 - 205	2.766	0.715054±14	312 - 313	3.605	0.714788±14
98 - 99	1.792	0.714974±14	206 - 207	2.781	0.715055±14	314 - 315	3.632	0.714806±16
100 - 101	1.815	0.714870±16	208 - 209	2.795	0.715088±16	316 - 317	3.659	0.714634±16
102 - 103	1.838	0.714076±16	210 - 211	2.810	0.714897±14	318 - 319	3.686	0.714914±14
104 - 105	1.861	0.714488±16	212 - 213	2.825	0.715074±16	320 - 321	3.713	0.714679±16
106 - 107	1.884	0.714851±16	214 - 215	2.839	0.715116±16	322 - 323	3.739	0.714509±14
108 - 109	1.906	0.714820±14	216 - 217	2.854	0.714865±16	324 - 325	3.766	0.714740±14
110 - 111	1.929	0.715247±14	218 - 219	2.868	0.714966±14	326 - 327	3.793	0.714602±14
112 - 113	1.952	0.715471±14	220 - 221	2.883	0.714800±16	328 - 329	3.820	0.714583±14
114 - 115	1.971	0.715266±14	222 - 223	2.898	0.714926±14	330 - 331	3.847	0.714377±16
116 - 117	1.990	0.715996±16	224 - 225	2.912	0.714837±14	332 - 333	3.873	0.714164±17
118 - 119	2.009	0.716447±16	226 - 227	2.927	0.715019±17	334 - 335	3.900	0.715670±14
120 - 121	2.027	0.716393±16	228 - 229	2.941	0.714830±16	336 - 337	3.927	0.714315±16
122 - 123	2.046	0.716007±14	230 - 231	2.956	0.714780±14	338 - 339	3.954	0.714131±16
124 - 125	2.065	0.716172±14	232 - 233	2.971	0.714742±11	340 - 341	3.980	0.714192±16
126 - 127	2.084	0.716015±14	234 - 235	2.985	0.714542±14	342 - 343	4.007	0.714210±16
128 - 129	2.103	0.715992±14	236 - 237	3.000	0.714511±37	344 - 345	4.034	0.714458±16
130 - 131	2.122	0.715992±14	238 - 239	3.014	0.714343±14	346 - 347	4.061	0.714703±14
132 - 133	2.141	0.715865±14	240 - 241	3.029	0.714585±16	348 - 349	4.088	0.714858±14
134 - 135	2.160	0.715826±13	242 - 243	3.045	0.714774±16	350 - 351	4.114	0.714608±14
136 - 137	2.179	0.715925±16	244 - 245	3.067	0.714772±16	360 - 361	4.257	0.714643±16
138 - 139	2.197	0.715991±14	246 - 247	3.088	0.714543±14	370 - 371	4.358	0.714916±16
140 - 141	2.216	0.715308±14	248 - 249	3.110	0.714812±16	380 - 381	4.446	0.714589±14
142 - 143	2.235	0.715517±17	250 - 251	3.131	0.714917±13	390 - 391	4.538	0.714460±16
144 - 145	2.254	0.715325±14	252 - 253	3.153	0.714591±17	400 - 401	4.633	0.713834±14
146 - 147	2.273	0.715497±16	254 - 255	3.174	0.714882±13	410 - 411	4.720	0.714280±14
148 - 149	2.292	0.715335±14	256 - 257	3.196	0.715077±14	420 - 421	4.806	0.714205±14
150 - 151	2.311	0.715735±14	258 - 259	3.217	0.714966±14	430 - 431	4.873	0.714788±14
152 - 153	2.330	0.715958±16	260 - 261	3.239	0.714756±16	440 - 441	4.965	0.714302±14
154 - 155	2.349	0.715909±17	262 - 263	3.260	0.714582±14	450 - 451	5.042	0.713736±14
156 - 157	2.367	0.716029±14	264 - 265	3.282	0.714637±14	460 - 461	5.115	0.713265±16
158 - 159	2.386	0.715992±16	266 - 267	3.303	0.714886±14	470 - 471	5.188	0.712946±16
160 - 161	2.405	0.716125±16	268 - 269	3.325	0.714543±16	480 - 481	5.258	0.713747±14
162 - 163	2.424	0.715878±14	270 - 271	3.339	0.714989±14	490 - 491	5.325	0.713886±16
164 - 165	2.443	0.716101±16	272 - 273	3.351	0.714407±16	500 - 501	5.392	0.714007±16
166 - 167	2.462	0.715802±14	274 - 275	3.363	0.714984±13	510 - 511	5.458	0.714081±14
168 - 169	2.481	0.715828±16	276 - 277	3.375	0.714619±17	520 - 521	5.525	0.714051±14
170 - 171	2.500	0.715653±16	278 - 279	3.387	0.714725±14	530 - 531	5.592	0.713833±14
172 - 173	2.519	0.715606±14	280 - 281	3.399	0.714781±14	540 - 541	5.659	0.713977±14
174 - 175	2.537	0.715576±14	282 - 283	3.411	0.714726±14	550 - 551	5.726	0.713680±16
176 - 177	2.556	0.715672±17	284 - 285	3.423	0.714950±14	560 - 561	5.792	0.713723±17
178 - 179	2.575	0.715795±14	286 - 287	3.435	0.714985±14	570 - 571	5.859	0.713780±16
180 - 181	2.591	0.715858±16	288 - 289	3.447	0.714959±14	580 - 581	5.926	0.713457±16
182 - 183	2.606	0.715395±14	290 - 291	3.459	0.714977±13	590 - 591	5.993	0.713593±14
184 - 185	2.620	0.715586±14	292 - 293	3.471	0.715026±14	600 - 601	6.060	0.713860±14
186 - 187	2.635	0.715528±14	294 - 295	3.483	0.714835±16	610 - 611	6.126	0.713203±16
188 - 189	2.649	0.715353±14	296 - 297	3.495	0.714959±17	620 - 621	6.193	0.712955±14
190 - 191	2.664	0.715483±16	298 - 299	3.507	0.714924±16	630 - 631	6.260	0.712775±14
192 - 193	2.679	0.715585±14	300 - 301	3.519	0.715195±17	640 - 641	6.327	0.713041±16

All ratios are normalized to $^{86}Sr/^{88}Sr = 0.1194$. The $^{87}Sr/^{86}Sr$ ratios of the NIST SRM-987 during the analysis are 0.710244±0.000023 (2σ, n = 11) for NP18 and 0.710252±0.000027 (2σ, n = 152) for NGC55 and NP29. The ratios of NP18 are normalized to the value of the NIST-SRM 987 for NGC55 and NP29.

* The error in the final digit ($2\sigma_m$) is given.

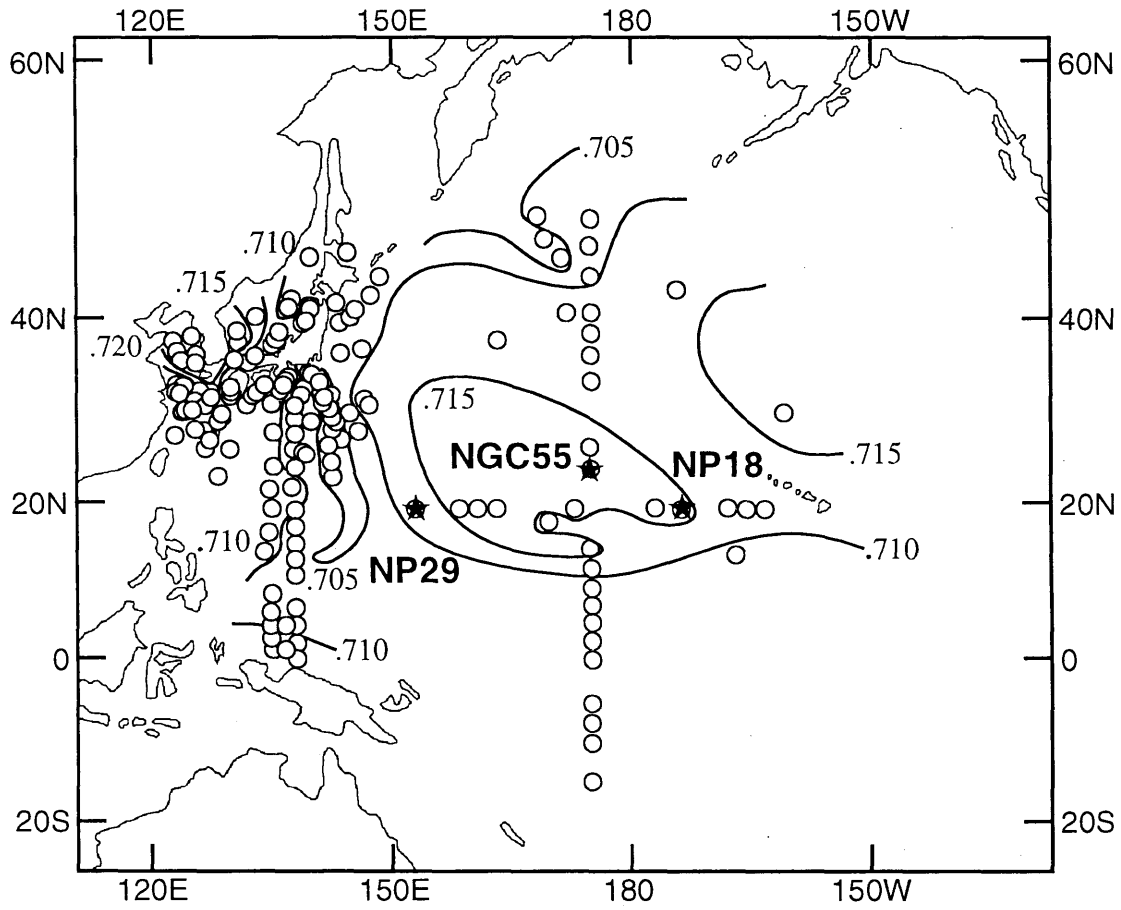

Fig. 1 Asahara

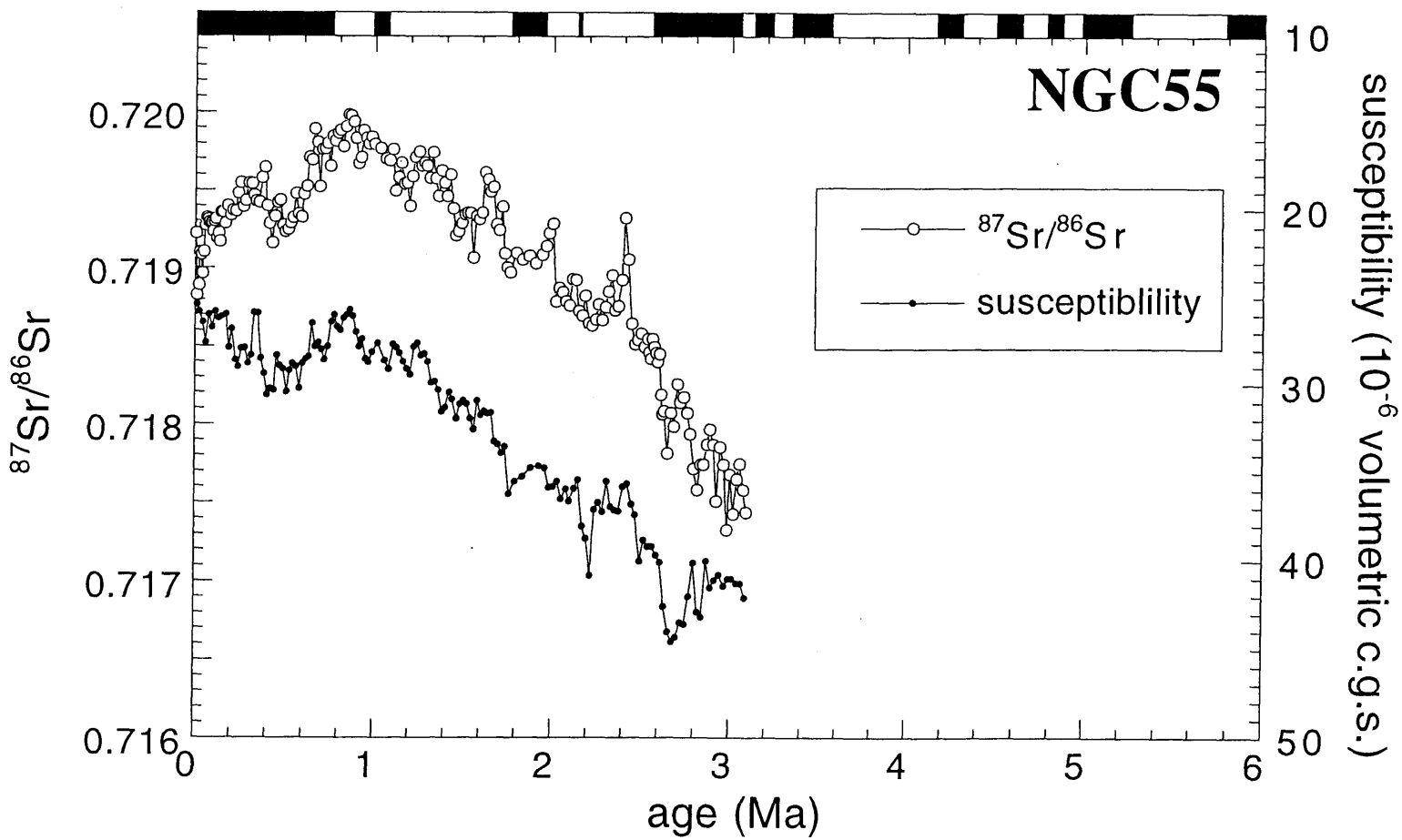

Fig. 2-a Asahara

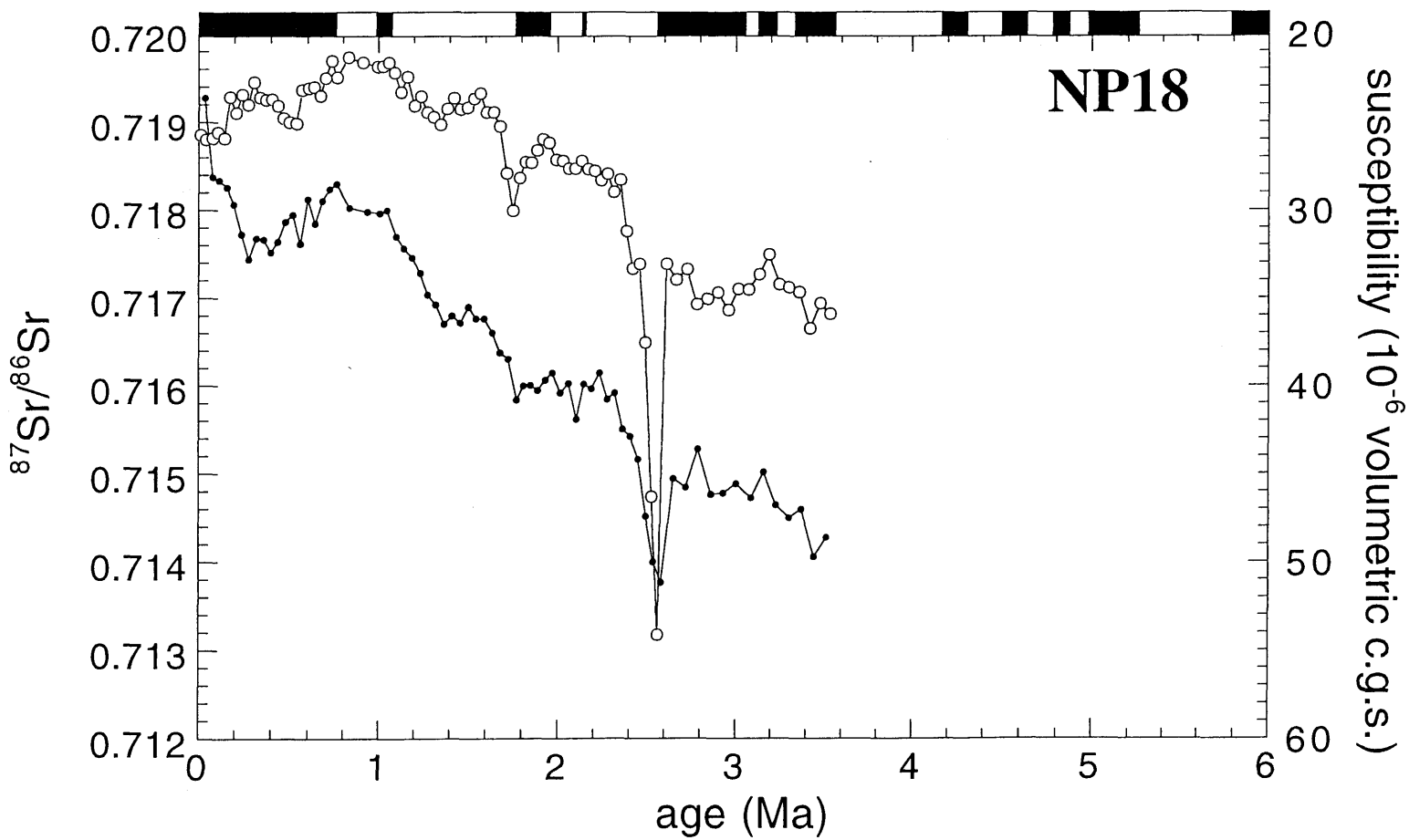

Fig. 2-b Asahara

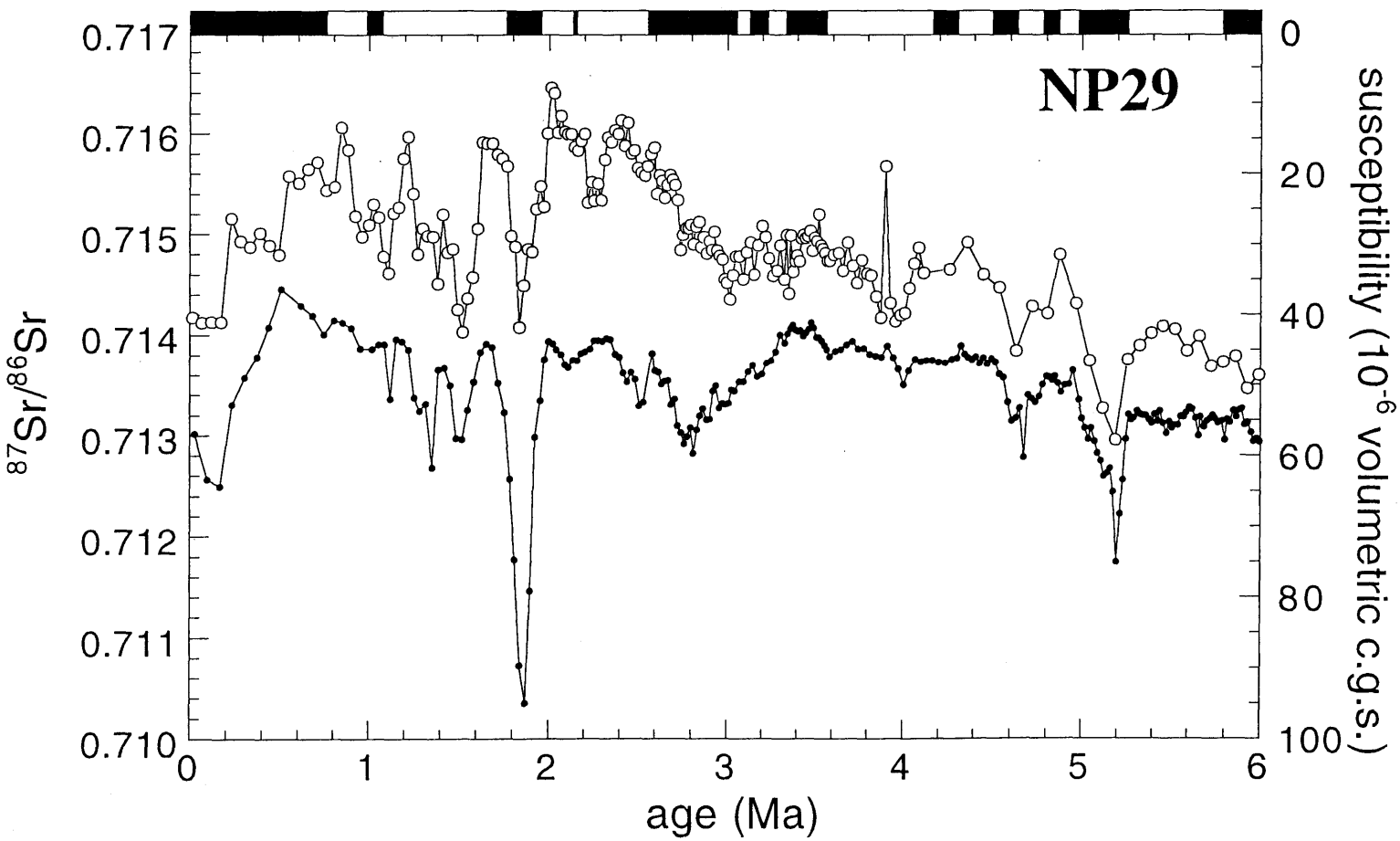

Fig. 2-c Asahara

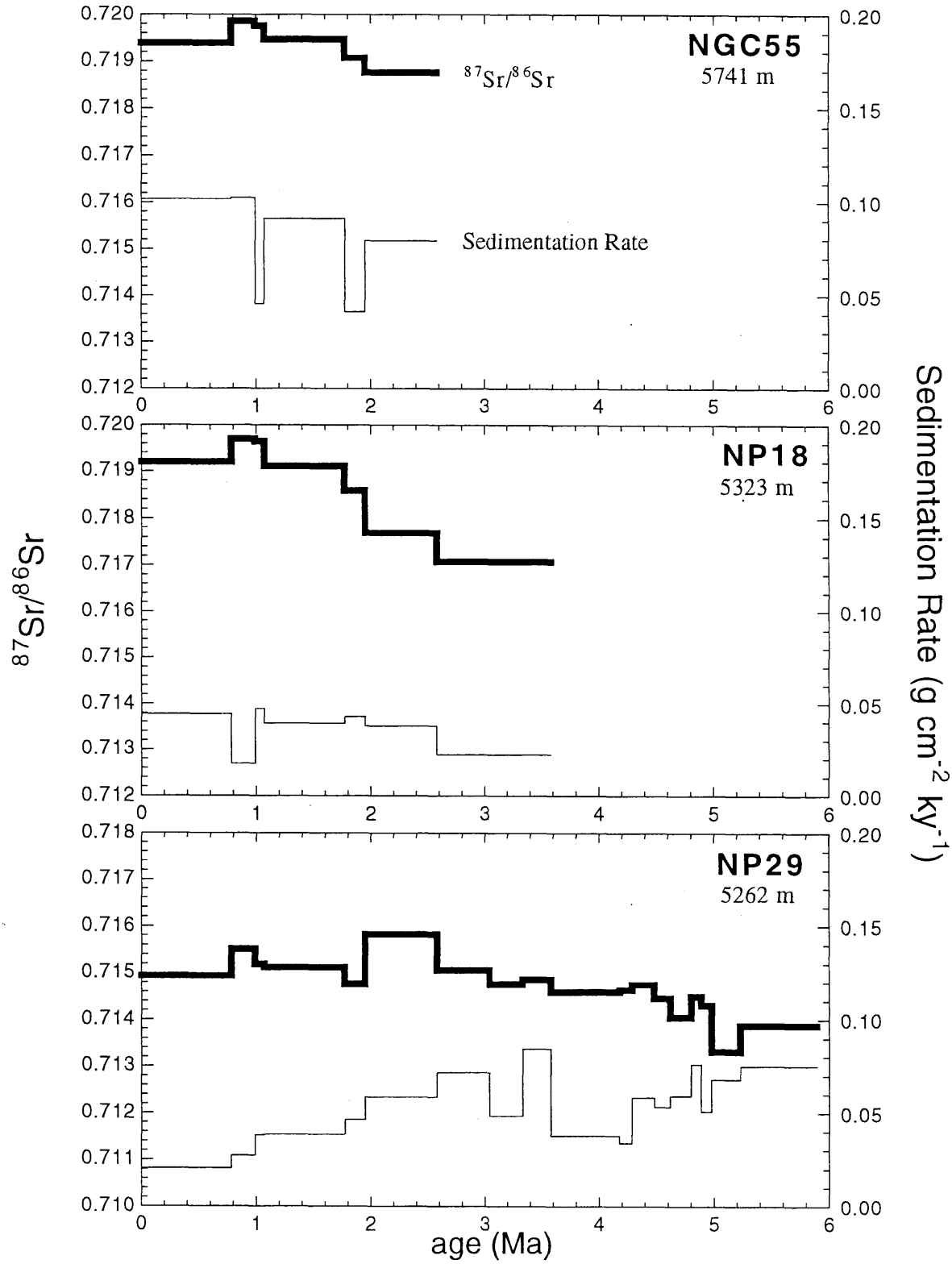

Fig. 3 Asahara

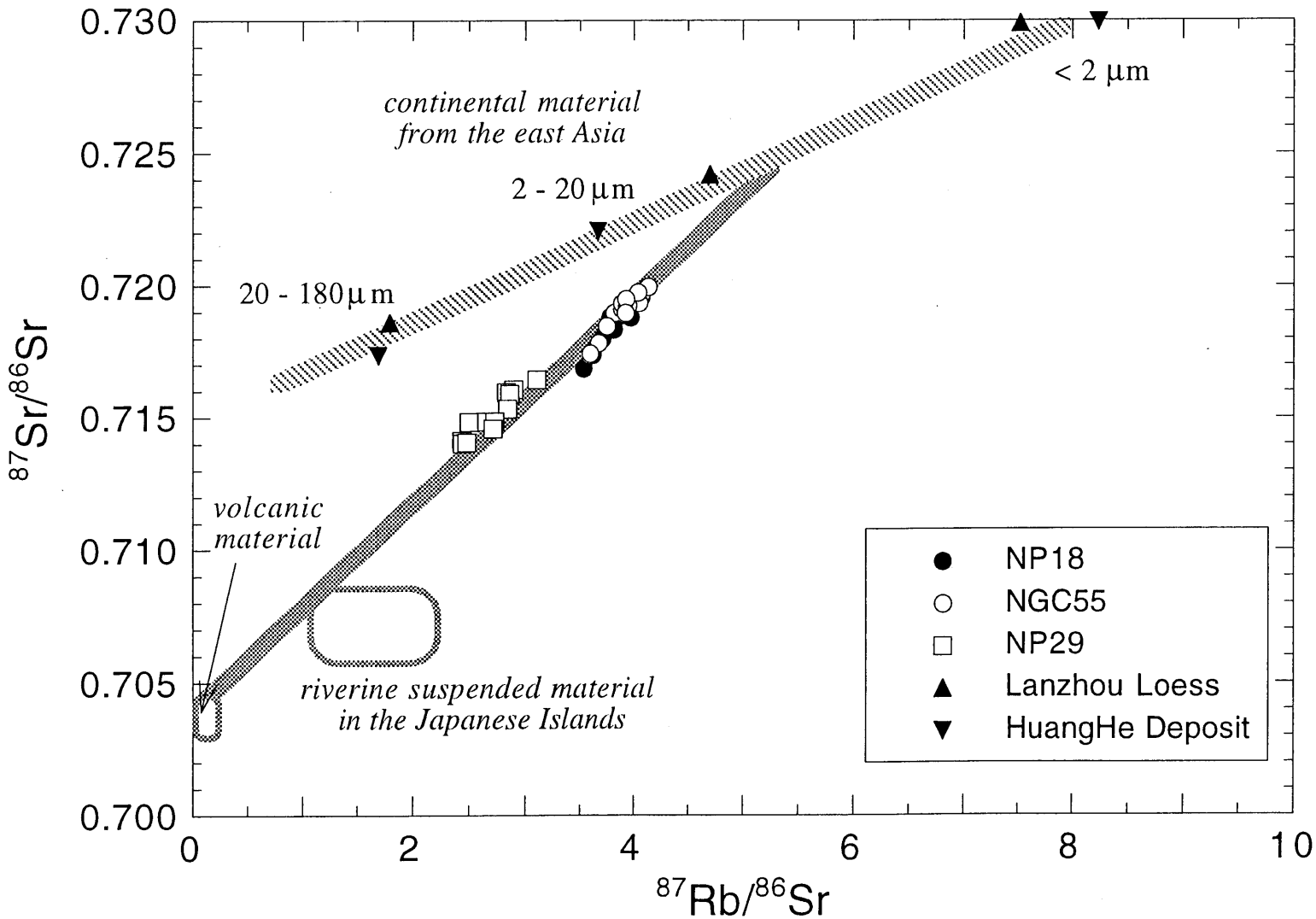

Fig. 4 Asahara

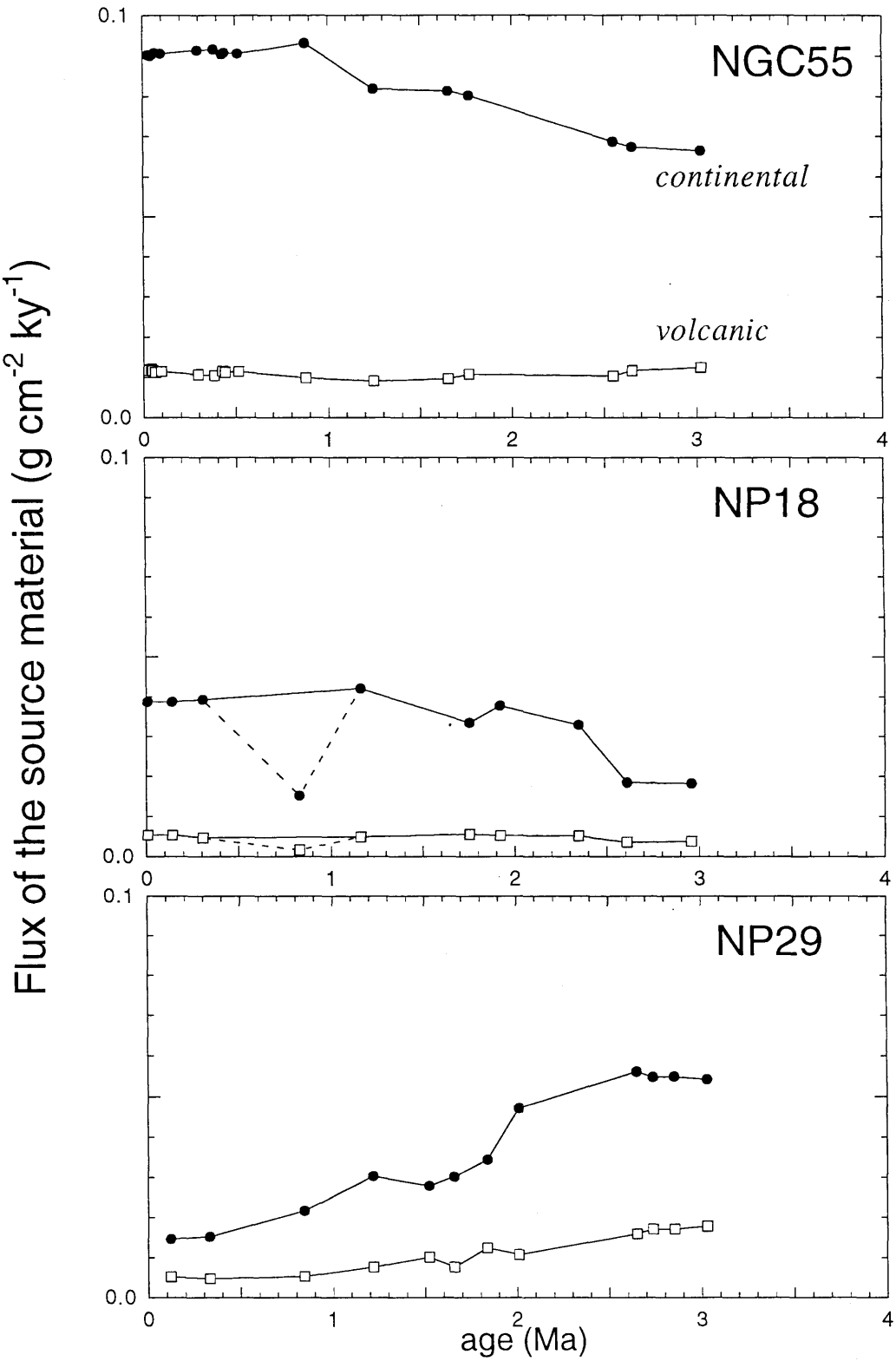

Fig. 5 Asahara

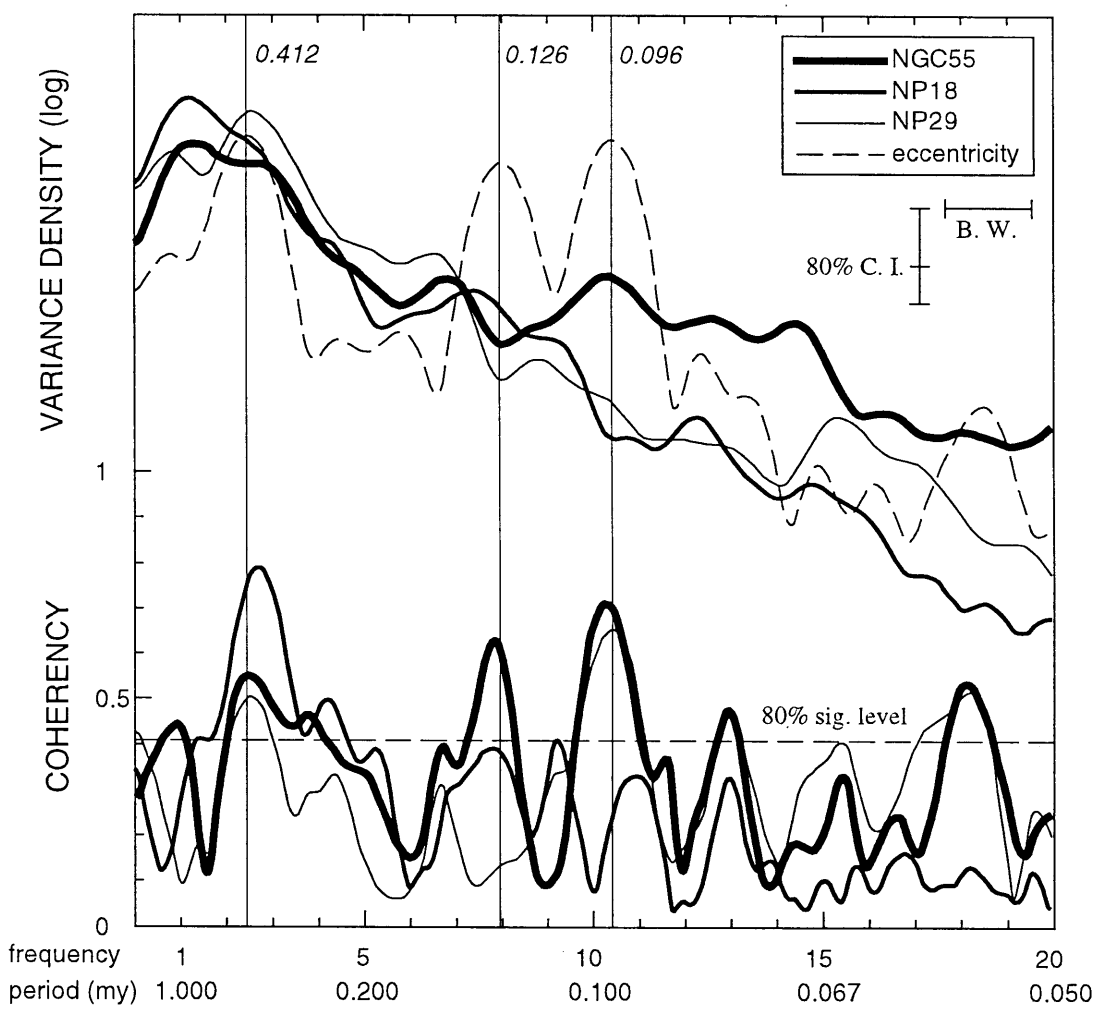

Fig. 6 Asahara

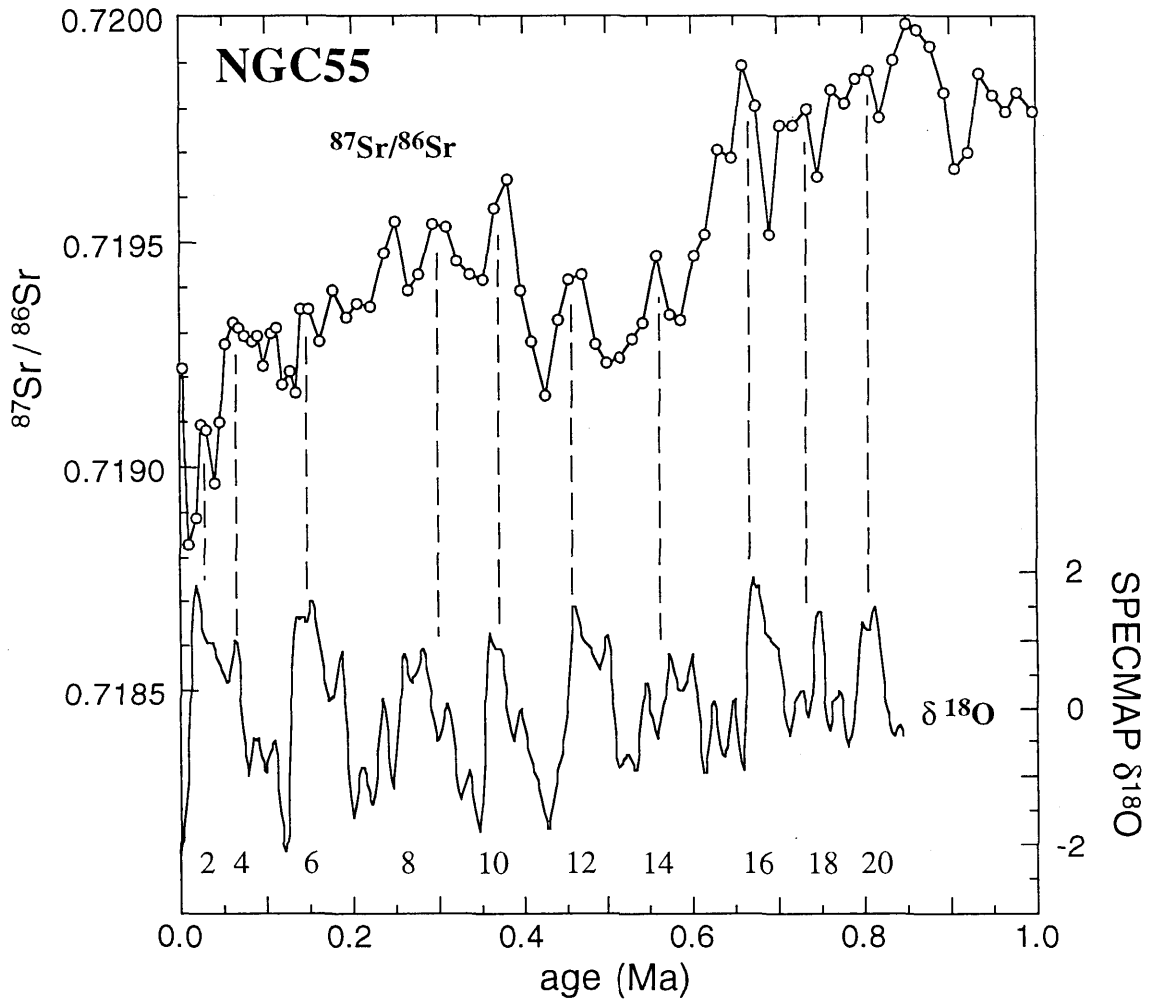

Fig. 7 Asahara

参考論文

1. Yoshihiro Asahara, Tsuyoshi Tanaka, Hikari Kamioka, Akira Nishimura and Toshitsugu Yamazaki (1999) Provenance of the north Pacific sediments and process of source material transport as derived from Rb-Sr isotopic systematics. *Chemical Geology* **158**, 271-291.

2. Yoshihiro Asahara, Tsuyoshi Tanaka, Hikari Kamioka and Akira Nishimura (1995) Asian continental nature of $^{87}Sr/^{86}Sr$ ratios in north central Pacific sediments. *Earth and Planetary Science Letters* **133**, 105-116.

3. 浅原良浩, 田中剛, 山本弘 (1995) α-HIBA を溶離液に用いたイオンクロマトグラフィーによる岩石中の希土類元素の分析. *岩鉱* **90**, 103-108.

4. 山本鋼志、田中剛、川邊岩夫、岩森光、平原靖大、浅原良浩、金奎漢、Chris Richardson、伊藤貴盛、Cristian Dragusanu、三浦典子、青木浩、太田充恒、榊原智康、谷水雅治、水谷嘉一、宮永直澄、村山正樹、仙田量子、高柳幸央、井上裕介、川崎啓介、高木真理、根布悟志、稲吉正実. 愛知県豊田市北東部の領家花崗岩地域の地球化学図. *地質学雑誌* **104**, 688-704.

5. Tsuyoshi Tanaka, Iwao Kawabe, Koshi Yamamoto, Hikaru Iwamori, Yasuhiro Hirahara, Koichi Mimura, Yoshihiro Asahara, Masayo Minami, Takamori Ito, Cristian Dragusanu, Noriko Miura, Hiroshi Aoki, Atsuyuki Ohta, Kaoru Togami, Takahiro Toriumi, Yoko Matsumura, Tomoyasu Sakakibara, Masahara Tanimizu, Yoshikazu Mizutani, Naozumi Miyanaga, Masaki Murayama and Yukio Takayanagi (1996) Geochemical Mapping of the northern area of Toyota City, Aichi Prefecture, Central Japan: Distinct chemical characteristics of stream sediments between granitic and sedimentary rock areas. *The Journal of Earth and Planetary Sciences Nagoya University* **43**, 27-47.

6. Tsuyoshi Tanaka, Masaharu Tanimizu, Yoshihiro Asahara, Chinatsu Yonezawa, Shigeko Togashi and Hikari Kamioka (1996) A variety of $^{143}Nd/^{144}Nd$ ratio among six high purity neodymium oxide reagents. *Journal of the Mass Spectrometry Society of Japan* **44**, 79-83.

7. Koshi Yamamoto, Yoshihiro Asahara, Hirokazu Maekawa and Kenichiro Sugitani (1995) Origin of blueschist-facies clasts in the Mariana forearc, Western Pacific. *Geochemical Journal* **29**, 259-275.

8. 田中剛、川邊岩夫、山本鋼志、岩森光、平原靖大、三村耕一、浅原良浩、伊藤貴盛、米澤千夏、ドラグシャヌ クリスチャン、神田聡、清水乙彦、林正人、三浦典子、青木浩、太田充恒、戸上薫、松村陽子、榊原智康、谷水雅治、水谷嘉一、宮永直澄、村山正樹、大森扶美子 (1995) 愛知県瀬戸市周辺における河川堆積物中の元素分布と地圏環境評価の試み. *地球化学* **29**, 113-125.

9. Tsuyoshi Tanaka, Iwao Kawabe, Yasuhiro Hirahara, Hikaru Iwamori, Koichi Mimura, Ryuichi Sugisaki, Yoshihiro Asahara, Takamori Ito, Hiroshi Yarai, Chinatsu Yonezawa, Satoshi Kanda, Otohiko Shimizu, Masato Hayashi, Noriko Miura, Keiko Mutoh, Atsuyuki Ohta, Koichi Sugimura, Kaoru Togami, Takahiro Toriumi and Yohko Matsumura (1994) Geochemical Survey of the Sanage-yama area in Aichi Prefecture for environmental assessment. *The Journal of Earth and Planetary Sciences Nagoya University* **41**, 1-31.